Structural, Spectroscopic and Angular-overlap Studies of the Nature of Metal-Ligand Bonding for Tripod Ligands *

Timothy Astley,[a] Allan J. Canty,[a] Michael A. Hitchman,[a] Graham L. Rowbottom,[a] Brian W. Skelton[b] and Allan H. White[b]

[a] *Chemistry Department, University of Tasmania, Hobart, Tasmania 7001, Australia*

[b] *Department of Physical and Inorganic Chemistry, University of Western Australia, Nedlands, W.A. 6009, Australia*

The metal(II) complexes $[M\{(pz)_2(py)CH\}_2][NO_3]_2$ (M = Fe, Co, Ni, Cu or Zn), where $(pz)_2(py)CH$ is the unsymmetrical tripodal nitrogen-donor ligand bis(pyrazol-1-yl)(pyridin-2-yl)methane, have been prepared and examined by single-crystal X-ray diffraction and single-crystal electronic spectroscopy. The structural studies, and the application of the angular overlap model to the spectroscopic results, provide new information on the bonding characteristics of tripod ligands and a comparison of pyrazole and pyridine groups. The zinc complex crystallizes in both the monoclinic ($P2_1/c$) and triclinic ($P\bar{1}$) systems, the monoclinic complex being isomorphous with those of cobalt and copper. The cations are centrosymmetric, but exhibit disorder in the orientation of the pyrazole and pyridine rings, except for the copper complex which exhibits a Jahn–Teller distortion involving two Cu–N (pz) bonds which are *ca.* 0.038 Å longer than the other Cu–N distances. Except for the copper complex, the ligands form 'bite' angles N–M–N of 83.8(2)–86.9(2)°, resulting in a slight trigonal distortion from octahedral geometry. The tripod ligand produces a relatively strong ligand field, consistent with the rather short metal–nitrogen bond lengths in the complexes. The pyridine group is a slightly stronger σ donor than the pyrazole groups, with both amines acting as weak π donors.

Tripod ligands containing nitrogen-donor heterocycles linked to a bridging carbon atom are widely used for a variety of applications in co-ordination and organometallic chemistry. For example, zinc(II) complexes of $(py)_3COH$ and $(mim)_3COH$, where Hpy = pyridine and Hmim = *N*-methylimidazole, are useful as models for some zinc-containing enzymes,[1] and the pyrazol-1-yl (pz)-containing ligand $(pz)_3CH$ has been of particular value in organometallic chemistry following Trofimenko's pioneering work in this area.[2] Ligands of this kind have been found to be particularly useful for stabilizing metals in both high and low oxidation states. Thus, $(py)_3CH$ and similar ligands form stable cobalt(I) complexes,[3] while $(pz)_3CH$, $(py)_3CH$ and related ligands have recently been found to stabilize high-oxidation-state organopalladium(IV) complexes to give the first example of a cationic complex for this oxidation state in $[PdMe_3(tripod)]I$.[4] Considerable interest has been shown in the relative importance of the electronic and steric characteristics of the ligands in influencing the oxidation state of the metal. For ligands such as $(py)_3P$ it was proposed[5] that low oxidation states may be stabilized by metal-to-atom ligand π-back bonding, this being facilitated by conjugation through the bridgehead atom. Such conjugation seems impossible for $(py)_3CH$, and it has been suggested[3] that the steric constraints of the ligand may somehow enhance the π-acceptor capacity of the amine rings compared with monodentate pyridine groups, helping to explain why ligands such as $(py)_3CH$ form stable cobalt(I) complexes, while pyridine itself does not. There has in fact been considerable controversy over the π-bonding properties of pyridine itself.[6]

As a contribution towards the elucidation of these questions, we have commenced a study of the structures and bonding properties of a range of complexes involving tripod ligands bonded to a transition-metal ions. The new tripod ligand bis(pyrazol-1-yl)(pyridin-2-yl)methane, $(pz)_2(py)CH$, has been chosen for initial studies since this should allow the metal–ligand bonding for the pyridine and pyrazole rings to be directly compared. In this report the crystal structures and electronic spectra of complexes formed by this ligand with iron(II), cobalt(II), nickel(II), copper(II) and zinc(II) nitrate are described, the angular overlap model (a.o.m.) being applied to derive metal–ligand bonding parameters where appropriate.

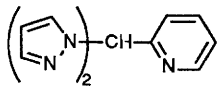

$(pz)_2(py)CH$

Experimental

The ligand $[(pz)_2(py)CH]$ was prepared as reported,[7] and its purity checked by microanalysis performed by the Canadian Microanalytical Service, Vancouver. Infrared spectra for KBr discs were measured with a Digilab FTS-200 FTIR spectrometer, and room-temperature magnetic susceptibilities were measured using a Johnson Matthey magnetic susceptibility balance calibrated with $(NH_4)_2Fe(SO_4)_2\cdot 6H_2O$.

Syntheses of Metal(II) *Complexes*.—$[Fe\{(pz)_2(py)CH\}_2][NO_3]_2$. A solution of iron(III) nitrate nonahydrate in acetone was added slowly with stirring to a solution of $(pz)_2(py)CH$ in acetone up to an $Fe^{III}:(pz)_2(py)CH$ molar ratio of 1:2. The precipitate was collected by filtration and recrystallized by vapour diffusion of diethyl ether into acetonitrile–methanol (1:1) solution. Red crystals formed slowly and were collected (yield 85%). The mechanism by which the metal was reduced in the formation of the compound is unknown. ν_{max} 3130, 2965,

---

* *Supplementary data available*: see Instructions for Authors, *J. Chem. Soc., Dalton Trans.*, 1991, Issue 1, pp. xviii–xxii.

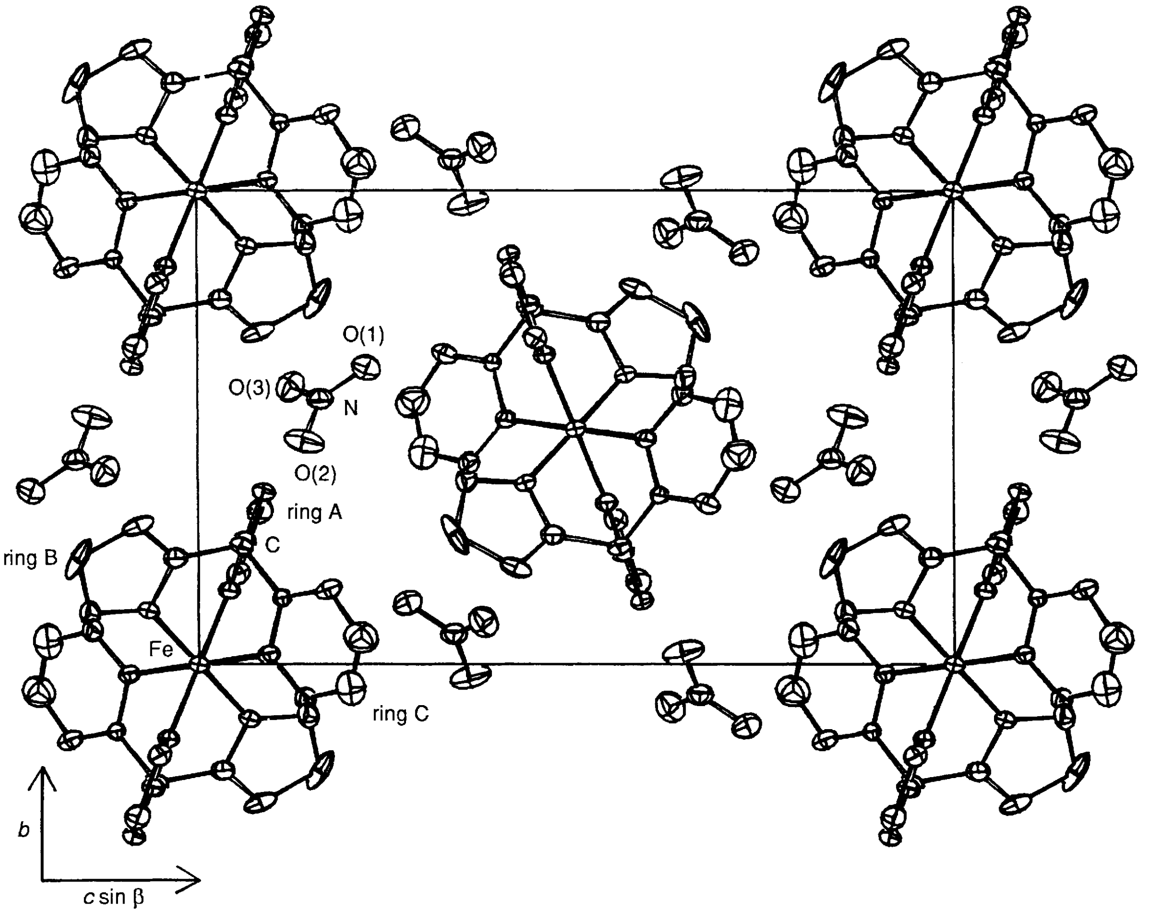

Fig. 1 Unit-cell contents of $[Fe\{(pz)_2(py)CH\}_2][NO_3]_2$ projected down *b*; 20% thermal ellipsoids are shown for the non-hydrogen atoms together with atom numbering. Hydrogen atoms have been omitted to improve clarity

1610, 1373, 1091 and 771 cm^{-1}; μ_{eff} 0.7_3 (Found: C, 45.7; H, 3.6; N, 26.8. Calc. for $C_{24}H_{22}FeN_{12}O_6$: C, 45.7; H, 3.5; N, 26.7%).

$[M\{(pz)_2(py)CH\}_2][NO_3]_2$ (M = Co, Ni, Cu *or* Zn). A solution of the hydrated metal(II) nitrate in acetone was added slowly with stirring to a solution of $(pz)_2(py)CH$ in acetone, with a M^{II}:$(pz)_2(py)CH$ mole ratio of 1:2. The precipitate formed was collected by filtration. Yields all $> \approx 95\%$. The cobalt(II) complex formed as yellow *crystals* on vapour diffusion of diethyl ether into acetonitrile–methanol (1:1) solution. ν_{max} 3125, 2961, 1609, 1391, 1063 and 773 cm^{-1}; μ_{eff} 4.9_0 (Found: C, 45.5; H, 3.5; N, 26.5. Calc. for $C_{24}H_{22}CoN_{12}O_6$: C, 45.5; H, 3.4; N, 26.7%). The nickel (II) complex formed as pink-purple *crystals* following a similar procedure to that used for the cobalt compound. ν_{max} 3109, 2977, 1609, 1392, 1063 and 773 cm^{-1}; μ_{eff} 3.0_1 (Found: C, 45.5; H, 3.5; N, 26.5. Calc. for $C_{24}H_{22}N_{12}NiO_6$: C, 45.6; H, 3.4; N, 26.8%). The zinc(II) complex formed as colourless *crystals* following a similar procedure; on inspection under a microscope it was found that the sample consisted of a mixture of two different crystalline forms, both of which were the subject of structure determination. ν_{max} 3133, 2969, 1607, 1379, 1063 and 773 cm^{-1} (Found: C, 45.1; H, 3.5; N, 26.3. Calc. for $C_{24}H_{22}N_{12}ZnO_6$: C, 45.2; H, 3.4; N, 26.5%). The copper(II) complex formed as blue *crystals* on vapour diffusion of diethyl ether into a solution of the complex in the minimum amount of acetonitrile. ν_{max} 3125, 2969, 1618, 1383, 1078 and 773 cm^{-1}; μ_{eff} 1.8_6 (Found: C, 45.2; H, 3.5; N, 26.3. Calc. for $C_{24}H_{22}CuN_{12}O_6$: C, 45.2; H, 3.4; N, 26.6%).

Structure Determinations.—For each complex a unique data set was measured at ≈295 K using an Enraf-Nonius CAD-4 diffractometer in conventional 2θ–θ scan mode with monochromatic Mo-Kα radiation (λ 0.7107_3 Å), yielding *N* independent reflections; N_o with $I > 3\sigma(I)$ were considered 'observed' and used in the full-matrix least-squares refinement after absorption correction, and solution of the structure by the heavy-atom method (Table 1). Anisotropic thermal parameters were refined for the non-hydrogen atoms and (x, y, z, U_{iso}) for hydrogen atoms were included constrained at estimated values, with reflection weights $\sigma^2(I) = \sigma^2(I_{diff}) + 0.0004\sigma^4(I_{diff})$. Neutral atom complex scattering factors were used;[8] computation used the XTAL 2.6 program system[9] implemented by Dr. S. R. Hall. Coordinates for the non-hydrogen atoms are given in Table 2, and details of the co-ordination geometries in Table 3. The zinc(II) complex occurs in monoclinic and triclinic forms, and the structures of the iron(II), nickel(II), copper(II) and triclinic zinc (II) complexes are illustrated in Figs 1–4.

Additional material available from the Cambridge Crystallographic Data Centre comprises H-atom coordinates, thermal parameters and remaining bond lengths and angles.

Individual abnormalities/variations in procedure. All the complexes are of stoichiometry $[ML_2][NO_3]_2$ with a complex cation and unco-ordinated nitrate counter ions. All are unsolvated with the possible exception of the triclinic zinc(II) complex (see below), and in every case the metal atom lies on a crystallographic inversion centre. Essentially ordered structures are proposed for the iron and copper compounds; in the remainder, some degree of disorder is apparent in the anion and/or cation, possibly of a concerted nature. The nitrate groups in the cobalt, nickel and monoclinic zinc compounds are disordered, with minor and major O_3 component arrays about the central nitrogen atoms. The cation disorder takes the form of some interchange between the pyrazole and pyridine rings, but with the centrosymmetric nature of the complex being retained in every case, so that the three ring atoms closest to the bridgehead carbon atom refine more 'satisfactorily' than the other ring atoms. An idealized representation of the overlap of

Table 1 Crystal data for metal(II) complexes $[M\{(pz)_2(py)CH\}_2][NO_3]_2$

Metal	Fe	Co	Ni	Cu	Zn (monoclinic)	Zn (triclinic)
Formula	$C_{24}H_{22}FeN_{12}O_6$	$C_{24}H_{22}CoN_{12}O_6$	$C_{24}H_{22}N_{12}NiO_6$	$C_{24}H_{22}CuN_{12}O_6$	$C_{24}H_{22}N_{12}O_6Zn$	$C_{24}H_{22}N_{12}O_6Zn\cdot 0.321\ H_2O$
M	630.4	633.5	633.2	638.1	639.9	645.7
Space group	$P2_1/c$	$P2_1/c$	$P2_1/n$	$P2_1/c$	$P2_1/c$	$P\bar{1}$
a/Å	8.109(5)	10.078(15)	10.268(3)	10.207(3)	10.129(3)	9.513(4)
b/Å	10.153(3)	8.017(3)	16.910(5)	7.756(2)	8.007(2)	8.965(4)
c/Å	16.774(7)	18.805(11)	7.907(2)	18.806(11)	18.788(9)	8.957(3)
β/°	106.43(4)	112.1(1)	90.15(2)	113.28(3)	112.15(3)	91.03(3)[a]
U/Å^3	1324.6	1407.8	1372.8	1367.7	1411.3	694.8
D_c/g cm^{-3}	1.58	1.49	1.53	1.55	1.51	1.54
Z	2	2	2	2	2	1
$F(000)$	648	650	652	654	656	333.2
μ_{Mo}/cm^{-1}	5.8	6.2	7.2	8.1	8.8	8.9
Crystal dimensions (mm)	0.10 × 0.29 × 0.27	0.55 × 0.42 × 0.35	0.28 × 0.18 × 0.16	0.45 × 0.24 × 0.14	0.16 × 0.14 × 0.14	0.30 × 0.18 × 0.15
$A^*_{min,max}$	1.10, 1.15	1.156, 1.224	1.08, 1.112	1.073, 1.158	1.100, 1.123	1.116, 1.183
$2\theta_{max}$/°	45	60	50	50	45	45
N	1730	3713	2407	2404	1839	1815
N_o, with $I > 3\sigma(I)$	1289	2036	1543	1840	1197	1540
R	0.054	0.068	0.068	0.047	0.059	0.048
R'	0.058	0.075	0.069	0.053	0.060	0.052

[a] $\alpha = 96.85(3)$, $\gamma = 113.31(3)$°.

pyrazole and pyridine rings is shown in Fig. 5, assuming bond angles for a pentagon and hexagon, respectively, and a geometry at C(2) and N(2) as expected for the free ligand. Larger thermal ellipsoids occur for the other carbon atoms, in particular C(4) for pyrazole rings and both C(4) and C(5) for pyridine rings, as here the effects of overlap are more pronounced. While libration effects should be most pronounced at the peripheries of the ligand rings, the thermal envelopes are in most cases excessive and irregular, and the disorder probably gives rise to the abnormal calculated bond lengths for these atoms, *e.g.* C(4)–C(5) (pz) bond lengths of 1.53(1) (ring b, Fe), 1.50(1) (ring b, Co), and 1.52(2) Å (ring b, Zn), and C(4)–C(5) (py) bond lengths of 1.19(2) (Fe), 1.19(1) (Co) and 1.20(2) Å (Zn).

Disorder is particularly evident in the triclinic zinc(II) complex, where it is great enough to allow a unique refinement of part of the pyridine/pyrazole moieties. In both pyrazole-ring environments pseudo-atom fragments appear between C(4A)/C(5A) and C(4B)/C(5B), namely C(45A) and C(45B) respectively (Fig. 4). Comparison of Fig. 4 with Fig. 5 indicates how the pseudo-atoms assigned as C(45A) and C(45B) arise, with these positions indicated as C(5)(py) in Fig. 5. This interpretation requires that the populations of C(45A), C(45B) and C(5) would be expected to be less than 1.000, and that the sum of the populations be equal to 1.000. Refinement of the populations of these atoms gave an approximate agreement with this model, with the sum of the occupancies of C(45A) [0.22(2)], C(45B) [0.34(2)] and C(5) [0.58(6)] within 3σ of 1.000. In this case the disorder may be connected with the presence of a difference-map artifact, possibly caused by the presence of lattice water molecules, modelled and refined as a partially occupied oxygen site, without the location of any associated hydrogen atoms. The cobalt, copper and monoclinic zinc compounds, which form a family with intermediate ⟨M–N⟩ distances, are isomorphous; among these, the copper complex is not disordered, presumably as a consequence of the distortion imposed by the Jahn–Teller effect. The zinc compound is the only member of the series to exist in two crystal forms; possibly the stability of the triclinic form is related to the fact that only in this case is solvent water present in the unit cell. Hydrogen atom coordinates (x, y, z) were refined for the nickel complex.

Results and Discussion

Crystal Structures of the Complexes.—Despite the disorder present in most of the complexes, resulting in rather higher than desirable residuals, the planarity of the ligand rings and the disposition of the ligands around the metal atoms is quite clear. It is this disposition which is of prime importance in the evaluation of the metal–ligand bonding parameters. It should be noted that the low absorption coefficients observed in the optical spectra of the nickel(II) and cobalt(II) complexes are consistent with the proposed nature of the disorder. If this disorder involved the presence of a proportion of complexes having a *cis* disposition of the pyridine rings, the non-centrosymmetric nature of these complexes would make the d–d transitions formally 'allowed', and the bands in the electronic spectra should be more intense.

Apart from the copper(II) complex, the tridentate ligands subtend 'bite' angles of 83.8(2)–86.9(2)° with the interligand N–M–N angle *ca.* 7° larger, resulting in a slight trigonal distortion from octahedral co-ordination geometry. The planes of the amine rings make angles of *ca.* 45° with those defined by the M–N bond vectors. The metal–ligand bond lengths are significantly shorter than those in complexes involving monodentate pyridine and pyrazole ligands, ≈2.066(5)–2.076(5) Å in the nickel complex, for instance, compared with ≈2.14 and ≈2.10 Å, respectively.[10,11] For all of the complexes the 'bite' of the tripod ligand and the geometry of the ligand results in an unsymmetrical orientation of each ring with the M–N direction. This effect is more pronounced for the pyrazole rings (Fig. 4), although a precise comparison of geometries is difficult owing to disorder. However, the angles M–N(1)–N(2) [117.1(5)–119.5(3)°] are substantially smaller than M–N(1)–C(5) [134.4(4)–138.4(6)°] for the pyrazole rings, with the ranges quoted excluding the highly disordered triclinic zinc(II) complex and the Jahn–Teller distorted copper(II) complex. The pyridine rings are more symmetrically disposed, exhibiting M–N(1)–C(2) about 7° smaller than M–N(1)–C(6) (Table 3).

Electronic Spectra.—The electronic spectrum of the nickel complex was measured at 290 and 15 K, by an experimental method described previously,[12] with the electric vector along the two extinction directions of the (010) crystal face, and the low-temperature spectrum is shown in Fig. 6. The band intensities are quite low, increasing somewhat at 290 K, in agreement with the centrosymmetric nature of the complex.[12] As expected for octahedrally co-ordinated nickel(II), in the region 8000–28 000 cm^{-1} the spectrum consists of two sets of

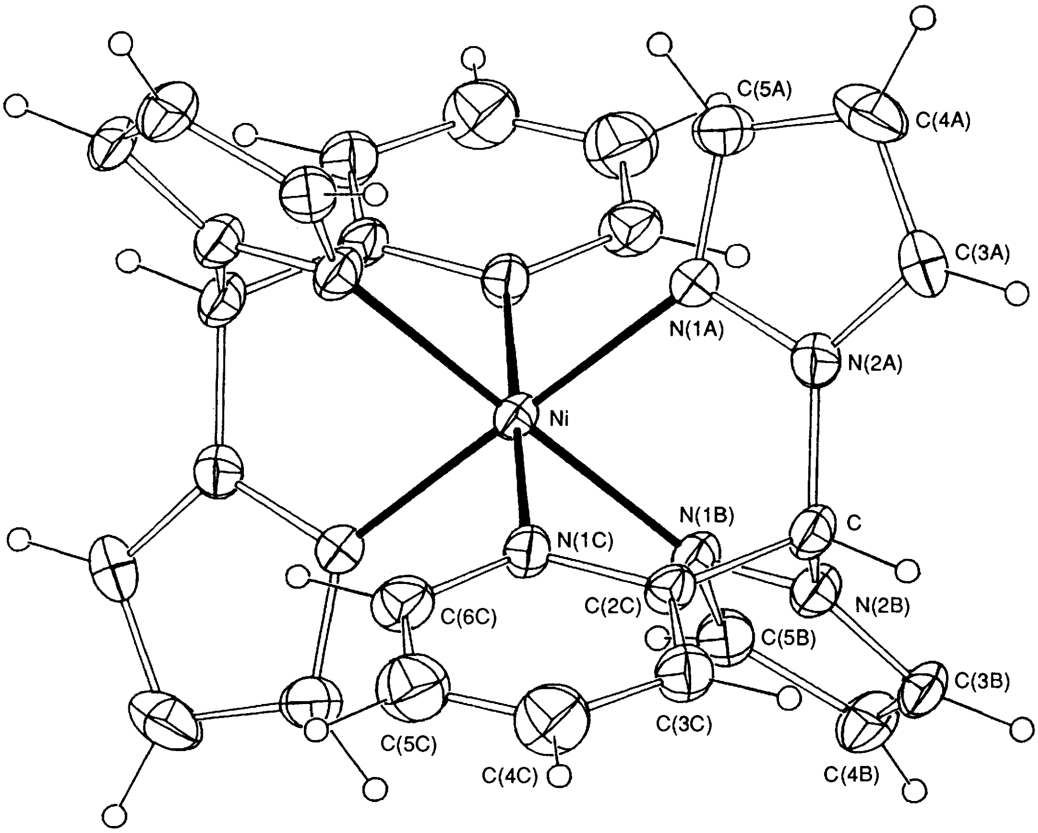

Fig. 2 Projection of the cation $[Ni\{(pz)_2(py)CH\}_2]^{2+}$ in the nitrate complex. Hydrogen atoms have been given an arbitrary radius of 0.1 Å

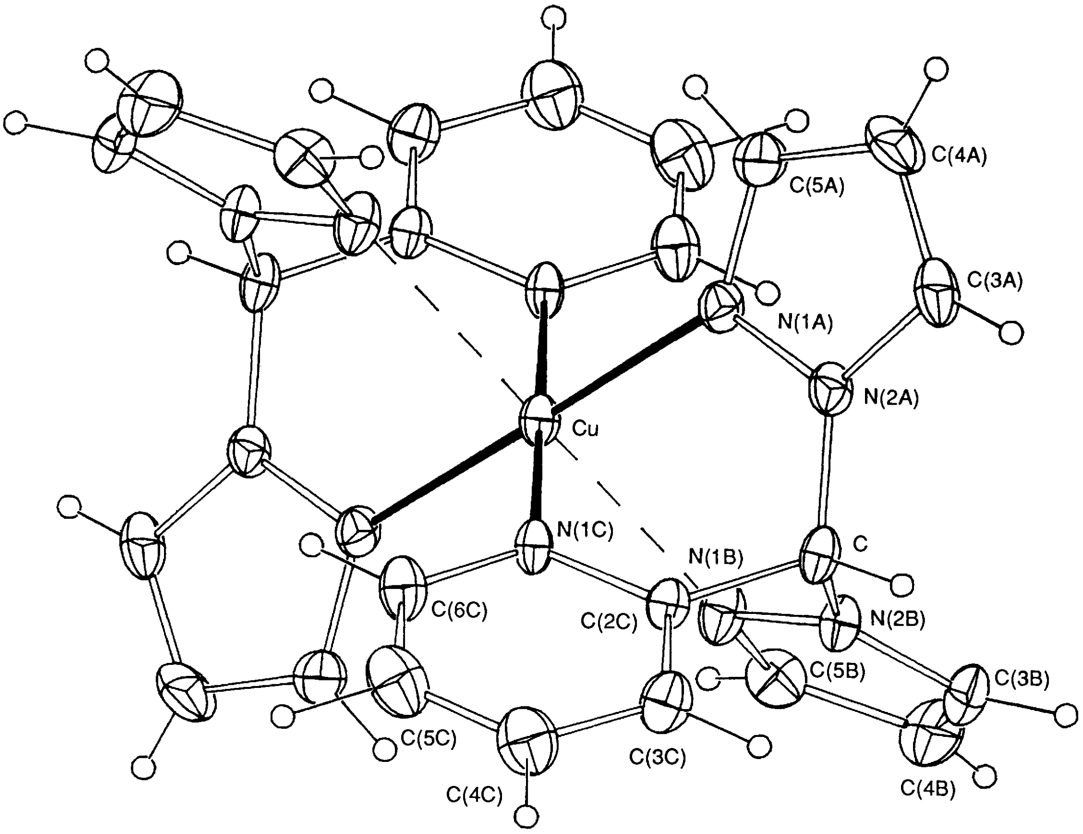

Fig. 3 Projection of the cation $[Cu\{(pz)_2(py)CH\}_2]^{2+}$ in the nitrate complex

spin-allowed peaks, centred at ≈13 000 and ≈20 000 cm^{-1}, each exhibiting splittings due to the low symmetry of the ligand field. The true symmetry of the complex is C_i, but if the primary co-ordination sphere alone is considered and the trigonal distortion is neglected the point group rises to D_{4h}. The transitions to the $^3T_{2g}$ and $^3T_{1g}$ levels of a regular octahedral nickel(II) complex are both split into three components in the former point group, and two in the latter. The second situation

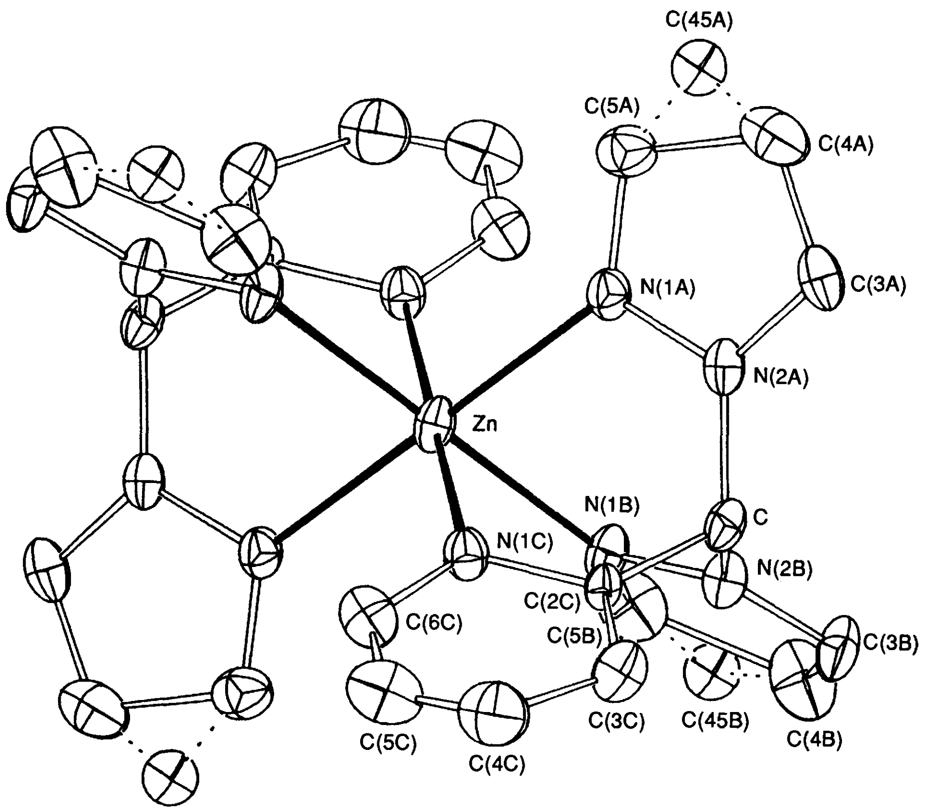

Fig. 4 Projection of the cation $[Zn\{(pz)_2(py)CH\}_2]^{2+}$ in the triclinic form of the nitrate complex, illustrating the disorder

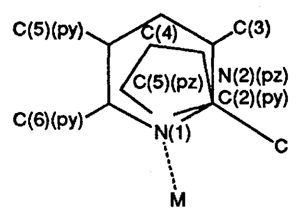

Fig. 5 Idealized overlap of pyrazole and pyridine rings, retaining the geometry expected for the free ligand, and showing the approximate position of the metal(II) ion in the complexes of Fe, Co, Ni and Zn

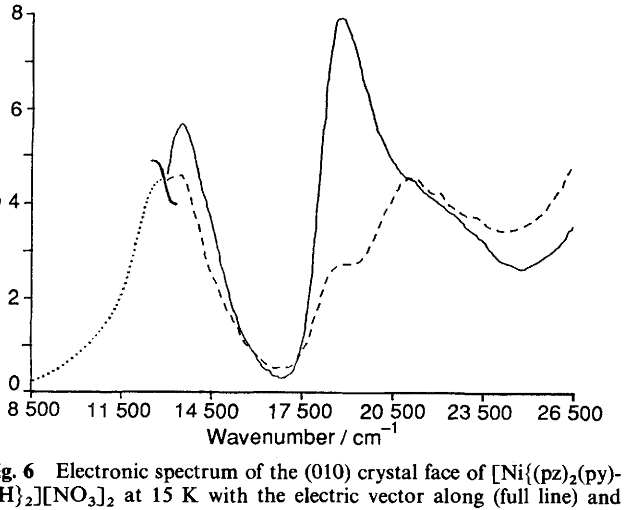

Fig. 6 Electronic spectrum of the (010) crystal face of $[Ni\{(pz)_2(py)CH\}_2][NO_3]_2$ at 15 K with the electric vector along (full line) and perpendicular (dashed line) to the [100] direction. If the molecular z axis is defined as lying along the direction of the Ni–N(pyridine) bonds, the squares of the projects made by the electric vector along this direction are 0.00 and 0.35 along these directions, respectively. The spectrum in the region below 13 000 cm^{-1} is for a KBr disk

is observed experimentally, and the energies of the band maxima are listed in Table 4 with the peaks assigned using

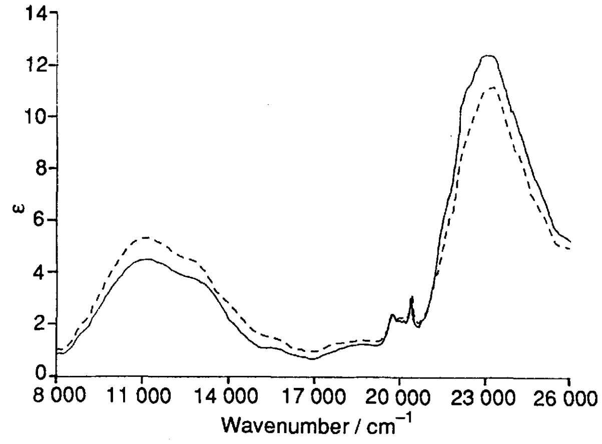

Fig. 7 Electronic spectrum of an arbitrary crystal face of $[Co\{(pz)_2(py)CH\}_2][NO_3]_2$ at 15 K with the electric vector along the two polarization directions

symmetry of labels of the D_{4h} point group (see caption to Fig. 6 for the z molecular projections associated with each spectrum). The relative weakness of the bands at 12 450 and 18 600 cm^{-1} when the electric vector is normal to [100] is also consistent with this approximation, as the transitions $^3A_{2g}$, $^3B_{2g} \longleftarrow {}^3B_{1g}$ are vibronically forbidden in z polarization in this point group. The electronic spectrum of an arbitrary crystal face of the cobalt(II) complex was also measured and this is shown in Fig. 7. The bands show splittings analogous to those observed for the nickel(II) complex and the assignments are given in Table 4.

The spectra associated with the two polarization directions of the (010) crystal face of $[Cu\{(pz)_2(py)CH\}_2][NO_3]_2$ in the range 1100–370 nm measured at 15 K are shown in Fig. 8. The dominant deviation of the ligand field from octahedral symmetry in this complex is the substantial lengthening of the bonds to two of the pyrazole ligands (Table 3), and the lowest-energy band may confidently be assigned to the transition between the components of the e_g levels split by this per-

Table 2 Non-hydrogen atom coordinates for $[M\{(pz)_2(py)CH\}_2][NO_3]_2$ and triclinic $[Zn\{(pz)_2(py)CH\}_2][NO]_3]_2 \cdot 0.321\ H_2O$; O(4,5,6) are disordered complements of O(1,2,3)[a]

	M = Co			M = Cu			M = Zn		
Atom	*x*	*y*	*z*	*x*	*y*	*z*	*x*	*y*	*z*
M	0	1	0	0	1	0	0	1	0
C	0.3026(4)	0.8544(7)	0.0872(2)	0.3005(4)	0.8489(6)	0.0904(2)	0.3042(8)	0.856(1)	0.0883(4)
N1A)	0.1948(4)	1.1274(5)	0.0547(2)	0.1856(3)	1.1245(4)	0.0463(2)	0.1962(7)	1.130(1)	0.0542(4)
N(2A)	0.3132(4)	1.0345(5)	0.0894(2)	0.3062(3)	1.0347(4)	0.0858(2)	0.3148(7)	1.0358(8)	0.0900(4)
C(3A)	0.4307(5)	1.1292(8)	0.1231(3)	0.4195(4)	1.1404(7)	0.1186(2)	0.4328(9)	1.128(2)	0.1248(6)
C(4A)	0.3865(7)	1.2948(9)	0.1104(4)	0.3694(5)	1.3056(6)	0.0997(3)	0.390(1)	1.293(2)	0.1125(7)
C(5A)	0.2374(6)	1.2848(7)	0.0669(3)	0.2237(4)	1.2889(6)	0.0547(2)	0.242(1)	1.286(1)	0.0681(6)
N(1B)	0.1191(4)	0.8306(5)	−0.0402(2)	0.1256(3)	0.7829(5)	−0.0374(2)	0.1222(6)	0.8292(9)	−0.0402(4)
N(2B)	0.2533(4)	0.7923(5)	0.0088(2)	0.2620(3)	0.7716(5)	0.0148(2)	0.2533(7)	0.7911(9)	0.0082(4)
C(3B)	0.3244(5)	0.6919(7)	−0.0229(3)	0.3470(4)	0.6912(6)	−0.0148(3)	0.3253(9)	0.691(1)	−0.0239(6)
C(4B)	0.2277(8)	0.6616(8)	−0.1012(4)	0.2627(6)	0.6485(7)	−0.0903(3)	0.229(1)	0.657(1)	−0.1024(7)
C(5B)	0.0963(6)	0.7582(7)	−0.1068(3)	0.1238(5)	0.7097(6)	−0.1017(2)	0.097(1)	0.753(1)	−0.1062(5)
N(1C)	0.0715(4)	0.8475(5)	0.0992(2)	0.0669(3)	0.8582(4)	0.0980(2)	0.0746(7)	0.8489(9)	0.1001(4)
C(2C)	0.2067(4)	0.7918(6)	0.1265(2)	0.2005(4)	0.7932(5)	0.1273(2)	0.2075(8)	0.793(1)	0.1254(4)
C(3C)	0.2496(6)	0.6808(8)	0.1836(3)	0.2426(4)	0.6827(6)	0.1880(2)	0.254(1)	0.683(1)	0.1840(6)
C(4C)	0.1570(8)	0.633(1)	0.2131(4)	0.1505(5)	0.6392(7)	0.2203(3)	0.161(2)	0.630(2)	0.2128(8)
C(5C)	0.0366(8)	0.683(1)	0.1909(4)	0.0224(5)	0.7060(7)	0.1940(3)	0.042(2)	0.686(2)	0.1905(9)
C(6C)	−0.0075(5)	0.7844(8)	0.1353(3)	−0.0169(4)	0.8107(6)	0.1336(2)	−0.006(1)	0.787(1)	0.1343(6)
N	0.3238(4)	1.1912(6)	0.2970(3)	0.3259(4)	1.1958(5)	0.2868(2)	0.323(1)	1.190(2)	0.2964(8)
O(1)	0.4292(5)	1.1142(8)	0.3202(5)	0.4278(4)	1.1021(6)	0.2993(3)	0.429(1)	1.113(1)	0.317(1)
O(2)	0.2127(5)	1.154(1)	0.2476(3)	0.2139(3)	1.1684(7)	0.2324(2)	0.217(1)	1.144(1)	0.2487(5)
O(3)	0.3238(7)	1.3223(9)	0.3292(5)	0.3393(4)	1.3149(6)	0.3327(2)	0.327(1)	1.319(2)	0.330(1)
O(4)	0.384(3)	1.172(3)	0.365(1)				0.395(6)	1.159(7)	0.370(3)
O(5)	0.371(3)	1.341(4)	0.287(2)				0.39(1)	1.33(1)	0.280(5)
O(6)	0.253(2)	1.078(3)	0.257(1)						

	M = Fe			M = Ni			M = Zn (triclinic)[b]		
M	1	0	0	1	1	1	0	0	1
C	0.8768(8)	0.2514(5)	0.0571(4)	0.7435(6)	0.9411(4)	0.849(1)	0.1764(5)	0.2840(5)	0.8171(5)
N(1A)	1.1383(6)	0.1576(4)	0.0409(3)	0.8769(5)	1.0603(3)	0.8380(7)	0.2183(4)	0.0592(5)	0.9036(4)
N(2A)	1.0580(6)	0.2626(5)	0.0615(3)	0.7665(5)	1.0220(3)	0.7851(8)	0.2693(4)	0.1903(4)	0.8277(4)
C(3A)	1.166(1)	0.3654(6)	0.0867(4)	0.6953(7)	1.0650(5)	0.6766(9)	0.3995(6)	0.2099(7)	0.7619(6)
C(4A)	1.327(1)	0.3243(7)	0.0820(4)	0.760(1)	1.1360(5)	0.652(1)	0.4434(7)	0.089(1)	0.7893(9)
C(5A)	1.3004(9)	0.1929(6)	0.0527(4)	0.8763(8)	1.1303(5)	0.755(1)	0.3149(8)	−0.0136(7)	0.8872(7)
N(1B)	0.8185(6)	0.1157(4)	−0.0658(3)	0.8346(5)	0.9629(3)	1.1258(8)	0.0794(5)	0.2589(4)	1.0665(5)
N(2B)	0.7767(7)	0.2258(5)	−0.0302(3)	0.7323(5)	0.9409(3)	1.0287(8)	0.1579(5)	0.3580(5)	0.9664(4)
C(3B)	0.6434(9)	0.2950(6)	−0.0796(5)	0.6314(6)	0.9158(4)	1.126(1)	0.2213(6)	0.5210(6)	1.0220(7)
C(4B)	0.5881(9)	0.225(1)	−0.1597(5)	0.6714(8)	0.9213(5)	1.290(1)	0.1857(8)	0.5463(9)	1.1642(9)
C(5B)	0.7118(9)	0.1087(7)	−0.1440(4)	0.7985(7)	0.9507(4)	1.283(1)	0.0825(7)	0.3499(9)	1.1940(7)
N(1C)	0.8964(6)	0.0209(5)	0.0921(3)	0.9705(5)	0.9025(3)	0.8448(7)	−0.0685(4)	0.0505(5)	0.7905(4)
C(2C)	0.8515(7)	0.1417(5)	0.1102(3)	0.8495(6)	0.8870(4)	0.7896(9)	0.0264(5)	0.1842(5)	0.7347(4)
C(3C)	0.7813(9)	0.1593(6)	0.1726(5)	0.8254(7)	0.8254(4)	0.681(1)	−0.0211(7)	0.2150(7)	0.6057(6)
C(4C)	0.758(1)	0.057(1)	0.2149(7)	0.925(1)	0.7802(6)	0.633(1)	−0.160(2)	0.107(2)	0.549(2)
C(5C)	0.801(1)	−0.051(1)	0.2005(6)	1.042(1)	0.7935(6)	0.692(1)	−0.238(3)	0.003(5)	0.591(2)
C(6C)	0.8685(9)	−0.0734(6)	0.1407(4)	1.0630(7)	0.8542(4)	0.793(1)	−0.1981(7)	−0.0265(7)	0.7046(8)
N	0.8020(9)	0.5646(6)	0.1620(4)	0.5668(8)	1.1639(6)	1.273(1)	−0.3616(8)	0.3418(7)	1.3704(8)
O(1)	0.8009(7)	0.6303(5)	0.2233(3)	0.6307(7)	1.2230(5)	1.301(1)	−0.2237(7)	0.4015(7)	1.3593(7)
O(2)	0.7011(8)	0.4732(5)	0.1406(4)	0.5936(9)	1.1253(5)	1.141(1)	−0.4185(6)	0.2601(6)	1.4667(6)
O(3)	0.9059(8)	0.5899(6)	0.1227(4)	0.4936(7)	1.1313(7)	1.370(1)	−0.4403(7)	0.3491(9)	1.2639(8)
O(4)				0.463(7)	1.189(4)	1.23(1)	0.340(4)	0.432(5)	1.497(4)
O(5)				0.553(9)	1.202(6)	1.37(1)			
O(6)				0.506(8)	1.172(5)	1.15(1)			

[a] Fractional nitrate oxygen populations are: Co, O(1,2,3), 0.860(4); O(4,5,6), 1 − 0.860(4); Zn (monoclinic), O(1,2) 0.89(2); O(4,5), 1 − 0.89(2); Ni, O(1,2,3), 0.9(−); O(4,5,6), 0.1(−). All O(4,5,6) were refined with isotropic thermal parameters. [b] In the zinc complex (triclinic), O(4) is water oxygen, population 0.32(2); disordered carbon components refined with isotropic thermal parameters were included and refined as C(45A) 0.422(4), −0.011(4), 0.835(3) and C(45B) 0.119(2), 0.481(2), 1.254(2), populations 0.22 and 0.34(2), respectively.

turbation. For complexes with π-donor ligands, tetragonally elongated along the *z* axis, the d_{xy} orbital is raised in energy with respect to d_{xz}, d_{yz}, and the shoulder observed at ≈15 000 cm^{-1} can therefore be assigned to the transition from the former orbital. In the present complex, the d_{xz}, d_{yz} orbitals will be split by the inequivalence of the in-plane ligands and it is this which presumably causes the highest-energy band to occur at a slightly different energy in the two polarizations. Although the true symmetry of the complex is C_i, if the primary co-ordination sphere alone is considered this rises to D_{2h}, and the assignments of the observed transitions using symmetry labels appropriate to this point group are given in Table 4.

The electronic spectrum in the visible region of a solution of the complex $[Fe\{(pz)_2(py)CH\}_2][NO_3]_2$ in methanol exhibits a single intense peak ($\varepsilon \approx 2000\ dm^3\ mol^{-1}\ cm^{-1}$) centred at 23 400 cm^{-1}. The spectrum of a crystal of the analogous zinc(II) complex containing a small concentration of Fe^{2+} ions measured at 15 K also exhibits this peak, as well as shoulders at ≈24 400 and 26 200 cm^{-1} (Fig. 9; the nature of the crystal face and space group of the zinc host were not investigated). These

Table 3 Bond distances and angles (°) for metal(II) and the bridgehead carbon in $[M\{(pz)_2(py)CH\}_2]^{2+}$

					Zn	
	Fe	Co	Ni	Cu	Monoclinic	Triclinic
M–N(1A,1A′)	1.963(5)	2.106(4)	2.066(5)	1.994(3)	2.132(6)	2.155(4)
M–N(1B,1B′)	1.961(4)	2.130(5)	2.068(5)	2.385(4)	2.163(8)	2.140(4)
M–N(1C,1C′)	1.967(5)	2.118(4)	2.076(5)	2.020(3)	2.121(7)	2.131(4)
⟨M–N⟩	1.96_4	2.11_8	2.07_0	2.13_3	2.13_9	2.14_2
'Intraligand' angles at metal[a]						
N(1A)–M–N(1B)	88.4(2)	86.4(2)	86.9(2)	86.7(1)	85.5(3)	84.9(2)
N(1A)–M–N(1C)	88.1(2)	84.5(2)	86.4(2)	86.8(1)	84.2(3)	83.8(2)
N(1B)–M–N(1C)	87.6(2)	83.9(2)	85.7(2)	81.8(1)	83.7(3)	84.7(2)
'Interligand' angles at metal[b]						
N(1A)–M–N(1B′)	91.6(2)	93.6(2)	93.1(2)	93.3(1)	94.5(3)	95.1(2)
N(1A)–M–N(1C′)	91.9(2)	95.5(2)	93.6(2)	93.2(1)	95.8(3)	96.2(2)
N(1B)–M–N(1C′)	92.4(1)	96.1(2)	94.3(2)	98.2(1)	96.3(3)	95.3(2)
Angles at nitrogen donor atoms						
M–N(1A)–N(2A)	117.7(4)	117.5(3)	117.4(4)	119.5(3)	117.1(5)	117.5(4)
M–N(1A)–C(5A)	135.9(4)	136.7(3)	137.2(5)	134.6(3)	138.4(6)	134.4(4)
M–N(1B)–N(2B)	119.2(3)	117.1(3)	116.6(4)	110.6(2)	117.5(5)	117.3(3)
M–N(1B)–C(5B)	133.4(4)	134.2(3)	137.4(5)	138.9(3)	133.7(5)	133.5(4)
M–N(1C)–C(2C)	118.7(4)	119.3(3)	118.8(4)	119.9(3)	119.1(6)	118.4(3)
M–N(1C)–C(6C)	126.4(4)	126.9(3)	124.8(5)	123.9(2)	124.9(6)	130.0(4)
Angles at the bridgehead carbon atom						
N(2A)–C–N(2B)	109.1(6)	111.3(4)	111.0(6)	110.8(3)	111.3(7)	111.3(4)
N(2A)–C–C(2C)	109.8(5)	111.8(4)	109.9(5)	111.4(3)	112.7(8)	111.7(4)
N(2B)–C–C(2C)	109.4(5)	110.2(4)	111.9(6)	111.3(3)	108.5(6)	111.3(4)

[a] Identical angles for primed ligand. [b] N(1A)–M–N(1B′) = N(1A′)–M–N(1B), *etc.*; N(1A)–M–N(1A′) = N(1B)–M–N(1B′) = N(1C)–M–N(1C′) = 180°.

Table 4 Metal–ligand bonding parameters, and calculated and observed transition energies and *g* values of the complexes. See text for the method of calculation

$[Ni\{(pz)_2(py)CH\}_2][NO_3]_2$

Transition	Observed	Calculated	
		I	II
$^3B_{1g}\rightarrow$			
$^3B_{2g}$	12 450	10 935	12 230
^3E_g	13 600	11 950	13 210
		12 270	13 300
$^1B_{1g}, ^1A_{1g}$	14 550	14 690	14 710
$^3A_{2g}$	18 600	16 920	18 420
^3E_g	20 900	19 755	21 450
		19 980	21 730
$^1A_{1g}$	≈25 000	24 210	24 635
	Bonding parameters		
	e_σ(py)	4 400	5 175
	$e_{\pi y}$(py)	1 020	1 020
	e_σ(pz)	4 500	4 820
	$e_{\pi y}$(pz)	600	645

$[Co\{(pz)_2(py)CH\}_2][NO_3]_2$

Transition	Observed	Calculated
$^4A_{2g}\rightarrow$		
^4E_g	10 800	10 650
		11 110
$^4B_{2g}$	12 000	11 850
$^2A_{2g}$	≈19 750	19 780
$^4B_{1g}$	≈20 000	19 980
^2E_g	≈20 100	20 875
	20 375	21 245
^4E_g	≈21 400	21 220
		21 410
$^4A_{2g}$	22 875	23 240
Bonding parameters*		
e_σ(py)		4 575
$e_{\pi y}$(py)		930
e_σ(pz)		3 930
$e_{\pi y}$(pz)		540
e_σ(pz)		4 200
$e_{\pi y}$(pz)		580

$[Cu\{(pz)_2(py)CH\}_2][NO_3]_2$

Transition	Observed	Calculated
$^2B_{1g}\rightarrow$		
$^2A_{1g}$	11 190	11 200
$^2B_{2g}$	15 085	15 080
^2E_g	17 200	17 140
	18 000	18 160
g_1	2.255	2.247
g_2	2.066	2.073
g_3	2.057	2.040
	Bonding parameters*	
	e_σ(py)	6 590
	$e_{\pi y}$(py)	1 300
	e_σ(pz)	5 540
	$e_{\pi y}$(pz)	740
	e_σ(pz)	500
	$e_{\pi y}$(pz)	100
	e_{ds}	775

* Two sets of bonding parameters were used for the pyrazole ligands, corresponding to the different metal–ligand bond lengths to these ligands.

bands are all probably due to metal-to-ligand charge-transfer transitions as similar peaks have been assigned[13] in this manner for Fe^{2+} ions doped into $[Zn(bipy)_3]^{2+}$ (bipy = 2,2′-bipyridine), though the possibility that the higher-energy shoulders are due to 'd–d' transitions cannot be ruled out, as the lowest-energy spin-allowed transitions are predicted to occur in this region. The nature of the charge-transfer excited states of the bipy complexes of iron(II) and ruthenium(II) have been the subject of detailed investigation because of their photochemical activity.[14]

It is interesting that the charge-transfer transition occurs at rather low energy in $[Fe\{(pz)_2(py)CH\}_2]^{2+}$ despite the fact that conjugation of the π systems of the amines over the whole ligand is hindered by the CH group of the tripod ligand. While

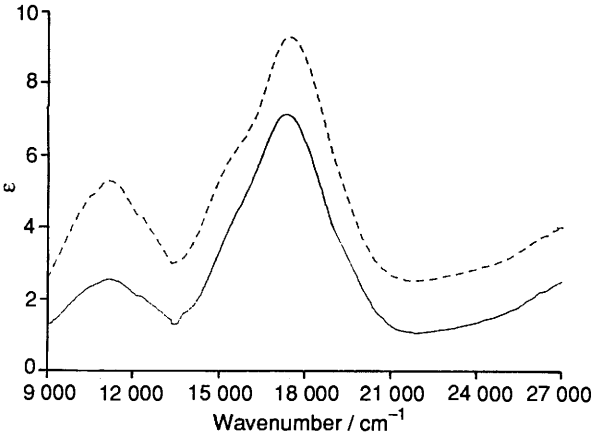

Fig. 8 Electronic spectrum of the (010) crystal face of $[Cu\{(pz)_2(py)CH\}_2][NO_3]_2$ at 15 K with the electric vector along (dashed line) and perpendicular (full line) to the [100] direction

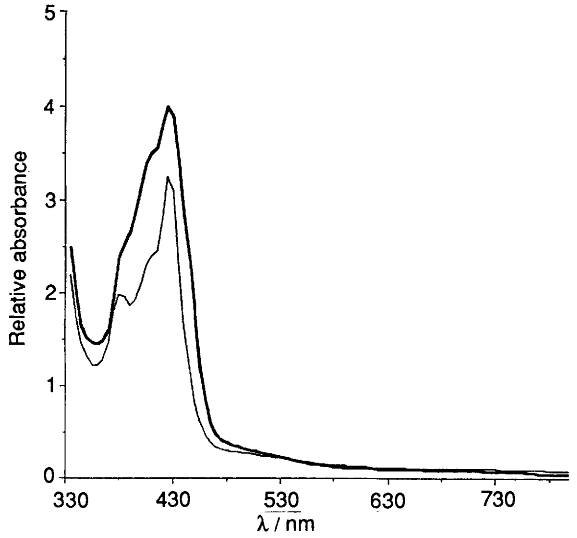

Fig. 9 Electronic spectrum of an arbitrary crystal face of a small percentage of Fe^{II} doped into $[Zn\{(pz)_2(py)CH\}_2][NO_3]_2$ at 15 K with the electric vector along the two polarization directions

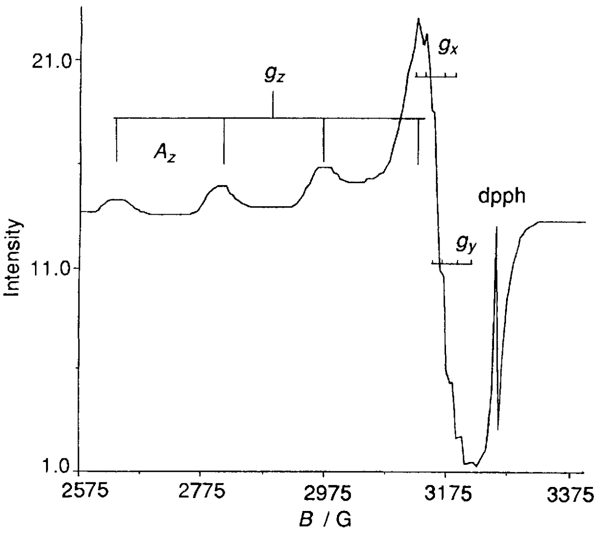

Fig. 10 The EPR spectrum of a frozen dimethyl sulphoxide solution of $[Cu\{(pz)_2(py)CH\}_2][NO_3]_2$; the sharp resonance at $g = 2.0036$ is due to a small amount of powdered diphenylpicrylhydrazyl (dpph) used as a reference marker; G = 10^{-4} T

the energy of the transition is higher than that for the complexes formed by the bipy ligand,[13] where such conjugation can occur ($\approx$23 400 compared with 19 000 cm^{-1}), it is somewhat lower than the onset of intense absorption in the spectra of complexes formed by monodentate pyridine ligands bound to iron(II) ($\approx$26 000 cm^{-1}).[15] Conceivably, the short bonds associated with the low-spin state of $[Fe\{(pz)_2(py)CH\}_2]^{2+}$ may influence the energy of the charge-transfer excited state, as the complexes formed by the monodentate amines are high spin. However, the charge transfer occurs at rather high energy ($\approx$29 000 cm^{-1}) in the low-spin complex $[Fe\{(pz)_3B\}_2]$.[16] Possibly the electron is donated to the pyridine rather than the pyrazole ring system in the excited state of $[Fe\{(pz)_2(py)CH\}_2]^{2+}$ and we intend investigating this aspect further by studying the iron(II) complexes formed by the symmetrical tripod ligands $(pz)_3CH$ and $(py)_3CH$.

EPR Spectrum of the Copper(II) Complex.—The EPR spectrum of a frozen dimethyl sulphoxide solution of $[Cu\{(pz)_2(py)CH\}_2][NO_3]_2$ (Fig. 10) indicates a slight orthorhombic distortion imposed upon basically axially symmetric g and copper hyperfine tensors and yields the following EPR parameters: $g_1 = 2.255$, $A_1 = 179 \times 10^{-4}$ cm^{-1}, $g_2 = 2.066$, $A_2 = 27 \times 10^{-4}$ cm^{-1}, $g_3 = 2.057$ and $A_3 = 29 \times 10^{-4}$ cm^{-1}.

The g values are in agreement with the metal–ligand bonding parameters derived from the electronic spectrum of the complex (see following section). The hyperfine parameters may be used to estimate the fractional unpaired spin density α^2 in the metal $d_{x^2-y^2}$ orbital using the relationships (1) and (2). Here, K, the

$$A_z = P[-K\alpha^2 - (4\alpha^2/7) + (3\,\Delta g_{xy}/7) + \Delta g_z] \quad (1)$$

$$A_{xy} = P[-K\alpha^2 + (2\alpha^2/7) + (11\,\Delta g_{xy}/14)] \quad (2)$$

isotropic Fermi parameter, has been estimated as 0.43, and the dipolar constant P, which is related to the average distance of a d electron from the nucleus, has been calculated to be 0.36×10^{-4} cm^{-1}.[17] Realistic results can only be obtained if A_z and A_{xy} are both negative, when substitution of the value of A_1 as A_z yields the estimate $\alpha^2 = 0.78$, and the average of A_2 and A_3 as A_{xy} gives $\alpha^2 = 0.86$. Since A_z can be measured more accurately, the former estimate is more reliable, and it agrees well with values deduced for other similar complexes[17] and with the orbital reduction parameter $k = 0.775$ estimated in the derivation of the bonding parameters of the complex (see following section).

Metal–Ligand Bonding Parameters.—The high energies of the 'd–d' transitions indicate that the tripod ligand produces a relatively strong ligand field, considerably stronger than monodentate pyridine or pyrazole groups, and comparable to 2,2′-bipyridyl and 1,10-phenanthroline [the lowest-energy transition occurs at $\approx$11 000 cm^{-1} for the hexa(pyrazole)nickel(II) complex,[18] and $\approx$12 200 cm^{-1} for the corresponding tris(2,2′-bipyridyl) complex[19]]. The high field strength of the latter ligand may be attributed to π-acceptor character related to the conjugation of the aromatic ring systems, but a similar explanation seems unlikely for the tripod ligand because of the presence of the bridgehead carbon atom. To investigate this point, the computer program CAMMAG, developed by Gerloch and co-workers,[20] was used to estimate the metal–ligand bonding parameters of the complexes within the framework of the angular overlap model (a.o.m.). This program calculates the transition energies of a complex, using as input the σ- and π-bonding parameters of the ligand donor atoms and the molecular geometry indicated by the crystal structure. In the present case this involves the parameters e_σ, $e_{\pi x}$ and $e_{\pi y}$ of the two amines, where $e_{\pi x}$ and $e_{\pi y}$ describe the π bonding parallel and perpendicular to the plane of the amine rings. To reduce the number of unknowns, $e_{\pi x}$ was set equal to zero for both amines, which is chemically reasonable in view of the fact that the p orbitals in the plane of each ring are fully involved in σ-bond formation. This approximation has been used previously in the determination of the a.o.m. bonding parameters of aromatic amines,[21] and it has been recently confirmed that the in-plane π-bonding parameters of monodentate pyridine and pyrazole ligands are indeed close to zero.[22]

Initially, the bonding parameters, derived[21] from the analysis of the optical spectra and magnetic susceptibilities of the complexes $[Ni(py)_4X_2]$ and $[Ni(Hpz)_4X_2]$ (py = pyridine; Hpz = pyrazole; X = Cl or Br) were used as estimates for the amine parameters in the calculations on $[Ni\{(pz)_2(py)CH\}_2]^{2+}$ (Table 4). However, the calculated transition energies (column 1 of Table 4) were significantly lower than those observed experimentally. The Ni–N bond lengths for the tripod ligand (2.076 and 2.067 Å for the pyridine and pyrazole groups, respectively) are significantly shorter than those for the monodentate amines in the above complexes (2.133 and 2.091 Å, respectively[11,23]). It has been observed[24] that, in agreement with theoretical predictions,[25] the ligand-field splitting in a complex is inversely proportional to approximately the fifth or sixth power of the metal–ligand bond length *r*, and recently such a relationship has been used to correlate the a.o.m. bonding parameters in several series of complexes involving similar ligands at different bond distances.[26] When bonding parameters corrected for the bond length differences assuming an r^{-6} dependence, as listed in Table 4, were used in the calculations the estimated transition energies agreed reasonably well with those observed experimentally, both as far as the overall position of the bands and the magnitudes of the band splittings are concerned (Table 4). Values of the Racah interelectron repulsion parameters of $B = 800$ and $C = 3800$ cm^{-1} were used in the calculations, with spin–orbit coupling being neglected. It may be noted that the calculated transition energies conform well to an approximate D_{4h} symmetry, *i.e.* for the split levels of both spin-allowed excited states, two levels are too close in energy to be resolved. The effect of varying the bonding parameters was investigated, and altering these significantly (more than ≈ 300 cm^{-1}) from the above values always produced a poorer fit with the observed transition energies. The optimum estimates of the bonding parameters are thus those derived previously for the corresponding monodentate amines, corrected for the shorter metal–ligand bond lengths observed for the tripod ligand.

A reasonable fit to the spectrum of $[Co\{(pz)_2(py)CH\}_2]^{2+}$ could be obtained using analogous bonding parameters to those used to fit the nickel spectrum, scaled to take into account the differences in bond length (Table 4). Similar slight differences have been observed in comparisons of the bonding parameters of analogous cobalt(II) and nickel(II) complexes.[27] Values of the Racah interelectron repulsion parameters $B = 725$ and $C = 3600$ cm^{-1} were used in calculating the cobalt(II) transition energies; a somewhat lower value of *B* is expected for the cobalt(II) complex than for the nickel analogue, because of the greater sensitivity of this parameter to the effective nuclear charge for the former metal ion.

Calculation of the energy levels of $[Fe\{(pz)_2(py)CH\}_2]^{2+}$ using Racah parameters $B = 800$ cm^{-1}, $C = 3200$ cm^{-1} and the metal–ligand bonding parameters derived for the nickel complex scaled for differences in metal–ligand bond lengths ($e_\sigma = 7240$ cm^{-1}, $e_\pi = 1470$ cm^{-1} for pyridine; $e_\sigma = 6620$, 6500 cm^{-1}, $e_\pi = 885$, 870 cm^{-1} for pyrazole) yields a spin-singlet ground state, in agreement with experiment, though with the spin-sextet state only 4300 cm^{-1} higher in energy. It would thus seem that the ligand-field strength of the tripod ligand is only just sufficient to stabilize a low-spin ground state. This agrees with the observation that iron(II) complexes with tripod ligands of the form $[(pz)_3BR]^-$ (R = pz), where pz may also be a substituted pyrazole, are sometimes high and sometimes low spin depending on the nature of the substituent.[16] Moreover, the analogous complex $[Co\{(pz)_2(py)CH\}_2][NO_3]_2$ is high spin. Complexes of iron(II) with monodentate pyridine and pyrazole ligands are invariably high spin, and it seems likely that the steric constraints of the tripod ligand, which favour short metal–ligand bond lengths, influence the adoption of the low-spin state in $[Fe\{(pz)_2(py)CH\}_2][NO_3]_2$.

Calculation of the transition energies of the copper(II) complex using the optimum parameters derived for the nickel(II) complex, scaled for the differences in bond length, produced rather poor agreement with experiment, particularly as far as the transition involving the d_{z^2} orbital is concerned. This is to be expected, both because the differences in bond length are substantial (Table 3), and configuration interaction with the metal 4s orbital is expected to depress the energy of the latter orbital in a complex with a large tetragonal distortion. However, reasonable agreement was obtained with only minor modification of the parameters of the in-plane ligands, using a value of the parameter $e_{ds} = 775$ cm^{-1} to account for the interaction with the metal 4s orbital (Table 4). Here, $4e_{ds}$ represents the energy by which the d_{z^2} orbital is lowered by this interaction.[28,29] The magnitude of e_{ds} seems reasonable, as this depends upon the difference between the axial and in-plane metal–ligand interaction,[28] being zero for a regular octahedral complex and rising to a value of ≈ 1500 cm^{-1} in planar complexes.[30] The depression of the d_{z^2} orbital from the energy predicted by simple bonding schemes has been investigated by Deeth and Gerloch[31] for copper(II) complexes having a wide range of tetragonal distortions. These authors interpret the depression in terms of an interaction with co-ordination voids, rather than d–s mixing, and infer a lowering in energy of ≈ 3500 cm^{-1} for axial bond lengths such as those in $[Cu\{(pz)_2(py)CH\}_2]^{2+}$, which is similar to the value deduced in the present study (≈ 3000 cm^{-1}). The *g* values calculated by CAMMAG agree reasonably well with those observed experimentally; the bonding parameters and *g* values are given in Table 4. The orbital reduction parameter used in the calculation, $k = 0.775$, is also similar to the value of $\alpha^2 = 0.78$ derived from the copper hyperfine parameter.

The amine groups in the tripod complexes are thus rather strong σ donors and moderate π donors, with the ligand-field strength following the sequence Fe > Cu > Ni > Co, which is also the order of increasing metal–ligand bond lengths. The parameters derived for the copper(II) complex ($e_\sigma = 6590$ cm^{-1}, $e_{\pi y} = 1300$ cm^{-1} and $e_\sigma = 5540$ cm^{-1}, $e_{\pi y} = 740$ cm^{-1} for the pyridine and pyrazole groups, respectively) agree well with those reported recently[22] for several planar copper(II) complexes formed by substituted pyridine and pyrazole ligands ($e_\sigma \approx 7000$ cm^{-1}, $e_{\pi y} = 900$ cm^{-1} and $e_\sigma \approx 6600$ cm^{-1}, $e_{\pi y} = 1070$ cm^{-1}, respectively), when the fact that the planar complexes have somewhat shorter Cu–N bond lengths is taken into account. As noted above, the bonding parameters of the nickel complex are somewhat higher than those in complexes with similar monodentate ligands, with the difference being attributable to the shorter metal–ligand bond lengths associated with the tripod ligand. The smallest bonding parameters in the series occur for $[Co\{(pz)_2(py)CH\}_2]^{2+}$; again, these are similar to, though somewhat higher than, the parameters derived for complexes involving analogous monodentate amines which have longer Co–N bonds (for instance the values $e_\sigma = 3700$ cm^{-1}, $e_{\pi y} = 100$ cm^{-1} have been reported[32] for the complex $[Co(py)_4Cl_2]$ in which the Co–N bond lengths are 2.183 Å;[33] the corresponding values in the tripod complex are $e_\sigma = 4650$ cm^{-1}, $e_{\pi y} = 900$ cm^{-1} for a Co–N length of 2.118 Å).

In agreement with previous studies on the analogous monodentate ligands,[22] the spectroscopic analysis suggests that the pyridine group in the tripod ligand produces a slightly stronger interaction than each pyrazole group. Although when considered in isolation the difference is probably too small to be significant, this conclusion is supported by several other lines of evidence. Thus, potentiometric and ^{1}H NMR studies indicate that pyridine groups are stronger σ donors than are pyrazole groups, at least for H$^+$ and the relatively simple organometallic cation $HgMe^+$ as acceptors.[34] Moreover, in the complex $[Cu\{(pz)_2(py)CH\}_2]^{2+}$ axial elongation occurs along bonds involving pyrazole, rather than pyridine groups. The fact that pyridine produces a stronger interaction with metal ions than pyrazole may also partly account for the higher stability of organopalladium(IV) complexes, $[PdMe_2R(tripod)]^+$, when the tripod ligand contains pyridine or *N*-methylimidazole rather than pyrazole groups.[4,35]

Conclusion

It is thus apparent that in the complexes $[M\{(pz)_2(py)CH\}_2]^{2+}$ (M = Fe, Co or Ni) the high ligand field is attributable to the rather short M–N bonds, presumably induced by the steric constraints of the ligand, rather than any π-acceptor character in the metal–ligand bonding. The strong σ-donor character of the ligand may help stabilize the unusual high oxidation state of palladium in $[PdMe_3\{(pz)_2(py)CH\}]^+$ and related complexes, although other factors are also involved.[4] However, such an effect clearly cannot explain the stability of the unusually *low* oxidation state of the metal in $[Co\{(py)_3CH\}_2]^+$. Conceivably, the bonding characteristics of the ligand may vary with the oxidation state of the metal, and we are currently investigating the metal–ligand bonding parameters in the series $[Co(tripod)_2]^{n+}$, n = 1, 2 and 3, to explore this possibility.

Acknowledgements

This work was supported by the University of Tasmania and the Australian Research Council, and we thank Dr. R. T. Honeyman for assistance with ligand synthesis. Dr. M. Gerloch, Cambridge University Chemical Laboratory, is thanked for making available the computer program CAMMAG.

References

1 See, for example, C. C. Tang, D. Davalian, P. Huang and R. Breslow, *J. Am. Chem. Soc.*, 1978, **100**, 3918; R. S. Brown and J. Huguet, *Can. J. Chem.*, 1980, **58**, 889.

2 See, for example, S. Trofimenko, *Chem. Rev.*, 1972, **72**, 497; *Prog. Inorg. Chem.*, 1986, **34**, 115.

3 T. A. Hafeli and F. R. Keene, *Aust. J. Chem.*, 1988, **41**, 1379.

4 P. K. Byers, A. J. Canty, B. W. Skelton and A. H. White, *J. Chem. Soc., Chem. Commun.*, 1987, 1093; P. K. Byers, A. J. Canty, B. W. Skelton and A. H. White, *Organometallics*, 1990, **9**, 826.

5 R. K. Boggess and D. A. Zatko, *Inorg. Chem.*, 1976, **15**, 626; R. K. Boggess and D. A. Zatko, *Inorg. Nucl. Chem. Lett.*, 1976, **12**, 7.

6 J. Glerup, O. Mønsted and C. E. Schäffer, *Inorg. Chem.*, 1976, **15**, 1399; 1980, **19**, 2855; D. W. Smith, *Inorg. Chem.*, 1978, **17**, 3153.

7 P. K. Byers, A. J. Canty and R. T. Honeyman, *J. Organomet. Chem.*, 1990, **385**, 417.

8 *International Tables for X-Ray Crystallography*, eds., J. A. Ibers and W. C. Hamilton, Kynoch Press, Birmingham, 1974, vol. 4.

9 The XTAL System, Technical Report TR-1364, eds., S. R. Hall and J. M. Stewart, Computer Science Center, University of Maryland, 1989.

10 C. W. Reimann, A. Santoro and A. D. Mighell, *Acta Crystallogr., Sect. B*, 1970, **26**, 521; C. W. Reimann, A. D. Mighell and F. A. Mauer, *Acta Crystallogr.*, 1967, **23**, 135; R. W. M. ten Hoedt, W. L. Driessen and G. C. Verschoor, *Acta Crystallogr., Sect. C*, 1983, **39**, 71.

11 G. J. Long and P. J. Clarke, *Inorg. Chem.*, 1978, **17**, 1394; F. Valach, P. Sivy and N. Koren, *Acta Crystallogr., Sect. C*, 1984, **40**, 957; D. J. Hamm, J. Bordner and A. F. Schreiner, *Inorg. Chim. Acta*, 1973, **7**, 637.

12 M. A. Hitchman, *Transition Metal Chemistry (New York)*, 1985, **9**, 1.

13 F. Felix, J. Fergusen, H. U. Güdel and A. Ludi, *Chem. Phys. Lett.*, 1979, **62**, 153.

14 J. Van Houten and R. J. Watts, *Inorg. Chem.*, 1978, **17**, 3381.

15 T. Astley and M. A. Hitchman, unpublished work.

16 J. P. Jesson, S. Trofimenko and D. R. Eaton, *J. Am. Chem. Soc.*, 1967, **89**, 3158.

17 M. A. Hitchman, *Inorg. Chem.*, 1985, **24**, 4762.

18 C. W. Reimann, *J. Phys. Chem.*, 1970, **74**, 561.

19 C. K. Jørgensen, *Absorption Spectra and Chemical Bonding*, Pergamon, Oxford, 1962, p. 124.

20 D. A. Cruse, J. E. Davies, M. Gerloch, J. H. Harding, D. Mackey and R. F. McMeeking, CAMMAG, a Fortran Computing Package, University of Cambridge, 1979.

21 A. Bencini, C. Benelli and D. Gatteschi, *Coord. Chem. Rev.*, 1984, **60**, 131; B. J. Kennedy, K. S. Murray, M. A. Hitchman and G. L. Rowbottom, *J. Chem. Soc., Dalton Trans.*, 1987, 825.

22 R. G. McDonald and M. A. Hitchman, *Inorg. Chem.*, 1990, **29**, 3074.

23 A. D. Mighell, A. Santoro, E. Prince and C. W. Reimann, *Acta Crystallogr., Sect. B*, 1975, **31**, 2479.

24 S. Minomura and H. G. Drickamer, *J. Chem. Phys.*, 1961, **35**, 903; H. G. Drickamer, *J. Chem. Phys.*, 1967, **47**, 1880.

25 D. W. Smith, *J. Chem. Phys.*, 1969, **50**, 2784; M. Bermejo and L. Pueyo, *J. Chem. Phys.*, 1983, **78**, 854.

26 R. G. McDonald, M. J. Riley and M. A. Hitchman, *Inorg. Chem.*, 1988, **27**, 894; R. G. McDonald and M. A. Hitchman, *Inorg. Chem.*, 1989, **28**, 3996.

27 D. M. L. Goodgame, M. A. Hitchman and B. Lippert, *Inorg. Chem.*, 1986, **25**, 2191.

28 D. W. Smith, *Inorg. Chim. Acta*, 1977, **22**, 107.

29 L. G. Vanquickenborne and A. Ceulemans, *Inorg. Chem.*, 1981, **20**, 796.

30 M. A. Hitchman and J. B. Bremner, *Inorg. Chim. Acta*, 1978, **27**, L61.

31 R. J. Deeth and M. Gerloch, *Inorg. Chem.*, 1984, **23**, 3853.

32 M. Gerloch, R. F. McMeeking and M. White, *J. Chem. Soc., Dalton Trans.*, 1976, 655; A. Bencini, C. Benelli, D. Gatteschi and C. Zanchini, *Inorg. Chem.*, 1980, **19**, 1301.

33 C. W. Reiman, A. D. Mighell and F. A. Mauer, *Acta Crystallogr.*, 1967, **23**, 135; G. J. Long and P. J. Clarke, *Inorg. Chem.*, 1978, **17**, 1394.

34 A. J. Canty and C. V. Lee, *Organometallics*, 1982, **1**, 1063.

35 P. K. Byers and A. J. Canty, *J. Chem. Soc., Chem. Commun.*, 1988, 639; D. G. Brown, P. K. Byers and A. J. Canty, *Organometallics*, 1990, **9**, 1231.

Received 27*th December* 1990; *Paper* 0/05802E